Universiteit Leiden
The Netherlands

Investigating metabolic disease in human induced pluripotent stem cells : apidocyte size, insulin signaling and hepatic lipids
Friesen, M.

Cover Page

Universiteit Leiden

The handle http://hdl.handle.net/1887/64936 holds various files of this Leiden University dissertation.

Author: Friesen, M.
Title: Investigating metabolic disease in human induced pluripotent stem cells : apidocyte size, insulin signaling and hepatic lipids
Issue Date: 2018-09-05

STEM CELLS AND REGENERATION   **TECHNIQUES AND RESOURCES REPORT**

Asialoglycoprotein receptor 1 is a specific cell-surface marker for isolating hepatocytes derived from human pluripotent stem cells

Derek T. Peters[1,2,*], Christopher A. Henderson[1,*], Curtis R. Warren[1,*], Max Friesen[1], Fang Xia[1], Caroline E. Becker[1], Kiran Musunuru[1,3] and Chad A. Cowan[1,4,‡]

ABSTRACT

Hepatocyte-like cells (HLCs) are derived from human pluripotent stem cells (hPSCs) *in vitro*, but differentiation protocols commonly give rise to a heterogeneous mixture of cells. This variability confounds the evaluation of *in vitro* functional assays performed using HLCs. Increased differentiation efficiency and more accurate approximation of the *in vivo* hepatocyte gene expression profile would improve the utility of hPSCs. Towards this goal, we demonstrate the purification of a subpopulation of functional HLCs using the hepatocyte surface marker asialoglycoprotein receptor 1 (ASGR1). We analyzed the expression profile of ASGR1-positive cells by microarray, and tested their ability to perform mature hepatocyte functions (albumin and urea secretion, cytochrome activity). By these measures, ASGR1-positive HLCs are enriched for the gene expression profile and functional characteristics of primary hepatocytes compared with unsorted HLCs. We have demonstrated that ASGR1-positive sorting isolates a functional subpopulation of HLCs from among the heterogeneous cellular population produced by directed differentiation.

KEY WORDS: Hepatocytes, Human pluripotent stem cells, FACS, MACS, Transcriptomics

INTRODUCTION

The hepatocyte mediates many liver functions by carrying out a multitude of activities at the cellular level. Despite the regenerative capacity of the liver *in vivo*, primary human hepatocytes (PHHs) are not viable *in vitro*, and they are in limited supply. Although micropatterned co-culture can extend the viability of PHHs *ex vivo* (Khetani and Bhatia, 2008), there is a substantial need for a renewable source of human hepatocytes for *in vitro* studies and the development of cell-based therapies. Human pluripotent stem cells (hPSCs) are a promising source of these cells (Schwartz et al., 2014).

There are well-established methods for the directed differentiation of hepatocytes from hPSCs using defined media and feeder-free culture conditions (Mallanna and Duncan, 2013). These protocols can be used to produce hepatocytes from hPSCs, generating a cellular population at least 70% positive for the hepatocyte-specific marker albumin. These cells also express other hepatocyte-specific genes and perform many of the hallmark cellular functions of hepatocytes, such as cytochrome activity and apolipoprotein secretion. However, hPSC-derived hepatocytes are not equivalent to primary adult human hepatocytes and are more accurately considered 'hepatocyte-like cells' (HLCs). Unlike adult hepatocytes, HLCs typically retain expression of the fetal hepatocyte marker alpha fetoprotein (AFP) and fall considerably short of mature hepatocytes in terms of quantifiable functional capabilities, such as albumin secretion and drug detoxification.

Substantial obstacles must be overcome before advanced disease modeling studies can be attempted with HLCs. One notable hurdle is the variability and inefficiency of differentiation (Bock et al., 2011; Osafune et al., 2008; Takayama et al., 2014). Evidence suggests that this characteristic variability stems from inherent differences in hPSC lines (Kajiwara et al., 2012). This problem poses a challenge for *in vitro* modeling of subtle phenotypes, as well as phenotypes that could be confounded by incomplete or inaccurate differentiation. Here we describe the validation of a strategy for the prospective isolation of HLCs differentiated from a variety of hPSC lines based on the expression of a liver-specific cell surface protein, ASGR1. ASGR1 has long been recognized as a hepatic surface marker (Ashwell and Morell, 1974; Schwartz et al., 1981) and has been used to identify circulating hepatocellular carcinoma cells (Li et al., 2014), purify hPSC-derived HLCs (Basma et al., 2009) and to demonstrate the efficiency of HLC differentiation from hPSCs (Takayama et al., 2014). Whereas the utility of ASGR1 as a marker of hepatocyte identity is well established, the subpopulation of cells expressing ASGR1 in hPSC-derived HLCs has not been rigorously studied on the transcriptional level. To improve our understanding of the ASGR1-positive subpopulation of hPSC-derived HLCs and in the interest of developing a strategy for the purification of functional HLCs, we extensively characterized ASGR1-positive cells. ASGR1 marks a subset of albumin-positive HLCs, which are more similar than unpurified cells to mature hepatocytes. Furthermore, we show that ASGR1-enriched HLCs can be replated for further functional analysis, while retaining hepatocyte marker expression and cellular functions for up to 72 hours after sorting. These purification strategies increase the utility of hPSC-derived HLCs by enabling the isolation of a homogeneous population of hepatocytes for functional studies.

RESULTS AND DISCUSSION
Directed differentiation of HLCs

Depending on the hPSC line used and other experimental variables, differentiation generally results in a mixture of HLCs (the desired cell type) and a variable number of other cell types (Fig. 1A). The specific composition of mixed HLC differentiation cultures has not been investigated. Our laboratory has developed an optimized HLC-directed differentiation protocol based on established methods (Pagliuca et al., 2014; Si-Tayeb et al., 2010) with modest modifications.

[1]Department of Stem Cell and Regenerative Biology and Harvard Stem Cell Institute, Harvard University, Cambridge, MA 02138, USA. [2]Harvard Medical School, Boston, MA 02115, USA. [3]Division of Cardiovascular Medicine, Brigham and Women's Hospital, Boston, MA 02115, USA. [4]Center for Regenerative Medicine, Massachusetts General Hospital, Boston, MA 02114, USA.
*These authors contributed equally to this work

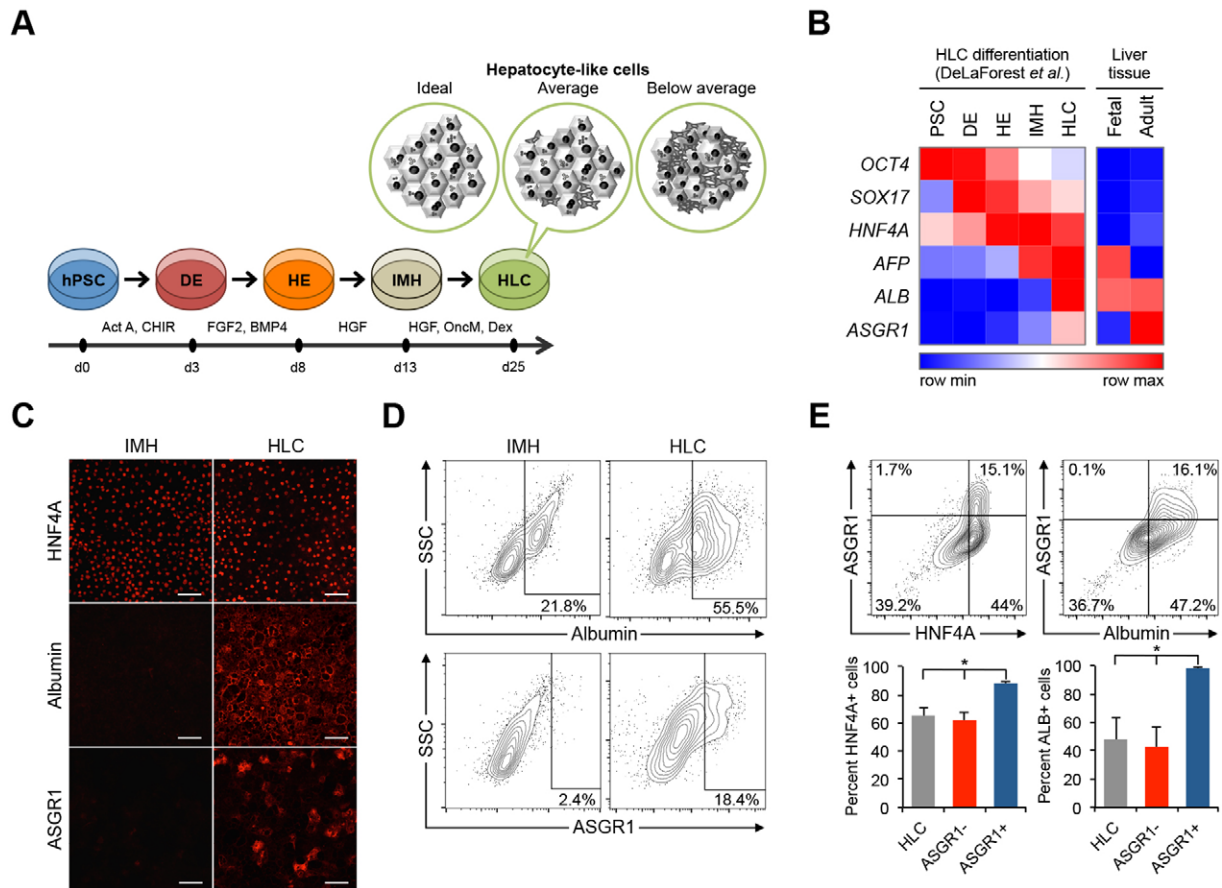‡Author for correspondence (chad_cowan@harvard.edu)

Fig. 1. Directed differentiation of hPSCs to hepatocyte-like cells (HLCs). (A) Overview of optimized protocol for directed differentiation from hPSCs to HLCs. Non-hepatic cell types contaminate the cell culture in suboptimal differentiation conditions. (B) Heatmap showing gene expression level of representative markers during each stage of HLC differentiation *in vitro* and in normal liver tissue *in vivo* from published microarray expression data (DeLaForest et al., 2011; Su et al., 2004). Expression values are row normalized; red denotes higher than average expression and blue denotes lower than average expression for each gene. (C) Confocal microscopy images of immunocytochemical staining after the third (IMH) and fourth (HLC) differentiation stages. Scale bars: 100 μm. (D) Representative flow cytometry analyses of ALB and ASGR1 expression at the IMH and MH differentiation stages. Similar patterns were observed in multiple independent differentiations (Fig. S1D). (E) Representative flow cytometry analyses showing co-expression of ASGR1 with HNF4α or ALB. Results of two independent differentiations per analysis are shown in the accompanying bar charts. Error bars represent s.e.m. *$P<0.05$, Student's *t*-test.

We analyzed published gene expression data from human tissues as well as from HLC differentiation of hPSCs and found that *ASGR1* is expressed in adult liver tissue, is not expressed or is present at an extremely low level in fetal liver, and is expressed most highly during HLC differentiation after the final differentiation stage – the 'HLC' stage (Fig. 1B). We confirmed this expression pattern during HLC differentiation by immunocytochemistry (Fig. 1C) and flow cytometry (Fig. 1D,E), which indicate that albumin (ALB) and ASGR1 are expressed at a very low level by a minority of cells at the end of the immature hepatocyte stage (IMH) and that they are both far more prevalent at the HLC stage of differentiation.

ASGR1 marks a subset of HLCs
Using our HLC differentiation protocol we found that ASGR1 is present in a small number of cells after the third differentiation stage (the IMH stage), and is more prevalent at the final stage of differentiation (Fig. 1D). This is in contrast to the expression pattern of the secreted protein ALB (a marker of functional hepatocytes), which is expressed at the IMH stage as well as the HLC stage (Fig. 1D).

The percentage of ASGR1-positive cells is almost always lower than that of ALB-positive cells in published reports as well as in our differentiations (Takayama et al., 2014). To confirm that ASGR1-

positive cells present at the end of HLC differentiation are in fact a subset of HLCs, we performed intracellular flow cytometry by co-staining for ASGR1 and other markers. We found that ASGR1-positive cells occur within a subpopulation of differentiated cells that express the hepatocyte lineage marker hepatocyte nuclear factor 4 alpha (HNF4α), as well as ALB (Fig. 1E).

Enrichment of differentiated hepatocytes based on ASGR1 surface expression
We next investigated the utility of ASGR1 for prospective hepatocyte isolation. We differentiated multiple human embryonic stem cell (hESC) and human induced pluripotent stem cell (hiPSC) lines representing a range of HLC differentiation propensities and characterized the expression of hepatocyte markers among cells positive for surface ASGR1. Fluorescence-activated cell sorting (FACS) analysis following HLC differentiation of four hPSC lines showed that a large proportion of surface ASGR1-positive cells were also ALB positive, even when the overall differentiation efficiency was extremely low (2.97% ASGR1-positive cells, Fig. 2A, summarized in Fig. 2B). Similar results were obtained when the expression of alpha-1 antitrypsin (AAT; SERPINA1 – Human Gene Nomenclature Committee), an additional marker of functional hepatocytes, was assessed (Fig. S2B).
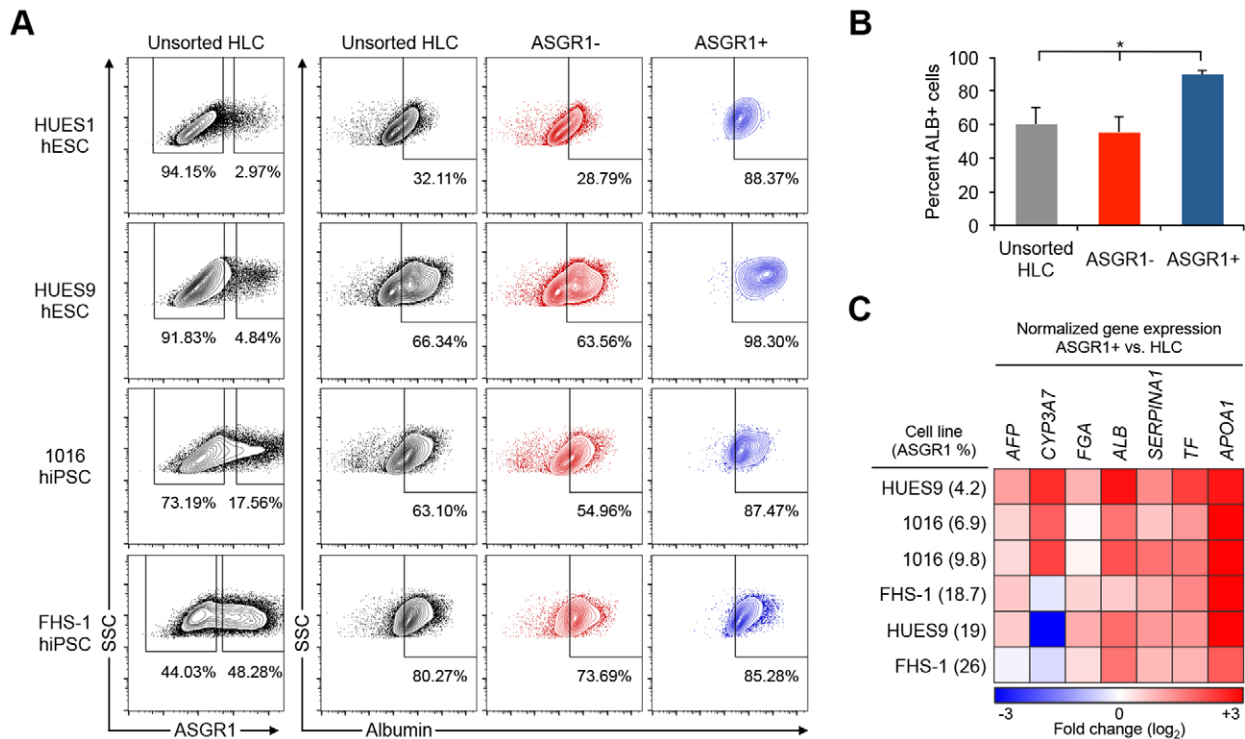
DEVELOPMENT

Fig. 2. Enrichment of hepatocytes from HLC differentiation cultures by surface ASGR1 FACS. (A) Four different hPSC lines were differentiated to HLCs. The percentage of cells expressing the hepatocyte marker ALB among unsorted HLCs, surface ASGR1-negative cells, and surface ASGR1-positive cells was quantified by intracellular flow cytometry. (B) Summary of results in A showing the mean percentage of ALB-positive cells by flow cytometry among unsorted HLCs, surface ASGR1-negative cells and surface ASGR1-positive cells (n=4 differentiations). Error bars represent s.e.m. *P<0.05, Student's t-test. (C) Heatmap summarizing qRT-PCR results, showing relative expression levels in ASGR1-positive cells compared with matched unsorted HLCs.

Next, we analyzed the expression of several hepatocyte-specific genes in unsorted HLCs and FACS-isolated ASGR1-positive cells from multiple differentiations of three representative hPSC lines. The average differentiation efficiency in these experiments ranged from 4.2% to 26% as measured by the percentage of ASGR1-positive cells (Fig. 2C, Fig. S2C). Particular hPSC lines generally differentiated well (e.g. FHS-1 hiPSC), whereas others differentiated with a lower efficiency (e.g. 1016 hiPSC), as expected based on prior studies of HLC differentiation propensity (Takayama et al., 2014). Hepatocyte marker genes, representing a range of *in vivo* expression patterns, from fetal expression (*AFP*) to adult liver expression [apolipoprotein A-I (*APOA1*)], were analyzed by qPCR (Su et al., 2004). We found that expression of hepatocyte marker genes was significantly higher in ASGR1-positive cells than in matched unsorted HLCs. This result was particularly pronounced for inefficient differentiations.

Global transcriptional profiling of ASGR1-positive cells

We next sought to confirm the identity of ASGR1-positive cells by global gene expression profiling. We analyzed the transcriptional profiles of matched samples of ASGR1-positive cells and unsorted HLCs differentiated from an hESC line (HUES9) and an hiPSC line (1016), as well as PHHs and HepG2 hepatoma cells (Knowles et al., 1980). Based on unbiased hierarchical clustering of all expressed genes, the global expression profiles of ASGR1-positive cells were distinct from those of matched unsorted HLCs (Fig. 3A). There was greater correlation between the expression profiles of ASGR1-positive cells from different hPSC lines (r^2=0.959) than there was between unsorted HLCs and ASGR1-positive cells from the same cell line (r^2=0.944) (P<0.05, Fig. S3A,B).

To further examine the effects of ASGR1 sorting, we performed differential expression analysis of the microarray data comparing ASGR1-positive cells with unsorted HLCs. We performed hierarchical clustering and heatmap visualization of all genes (probe sets) differentially expressed at a false discovery rate (FDR) of 5% (Fig. S3C) as well as of the most highly differentially expressed genes (>2-fold difference in expression between ASGR1-positive cells and HLCs, Fig. S2C). From this analysis we observed that ASGR1-positive cells cluster more closely to PHHs than to unsorted HLCs, whereas unsorted HLCs cluster more closely to HepG2 cells than PHHs.

A paired-sample design was used for differential expression analysis to characterize the gene expression profile of ASGR1-positive cells. This analysis identified genes differentially expressed in ASGR1-positive cells relative to matched HLCs differentiated from two different hPSC lines. 766 genes were differentially expressed more than 2-fold between ASGR1-positive cells and HLCs. Of these, 330 genes were significantly more highly expressed in ASGR1-positive cells versus unsorted HLCs (Fig. S3C). Functional enrichment analysis of the genes more highly expressed in ASGR1-positive cells was performed using the PANTHER classification system (Mi et al., 2013). Statistical overrepresentation analysis revealed overrepresentation of a number of hepatocyte-related gene ontology (GO) biological processes in ASGR1-positive cells versus unsorted HLCs (Fig. S3D). Many of the overrepresented processes related to key metabolic functions performed by the liver.

Next, we assembled a panel of hepatocyte genes representing important categories of hepatic function: synthetic function (including the production of coagulation factors), energy
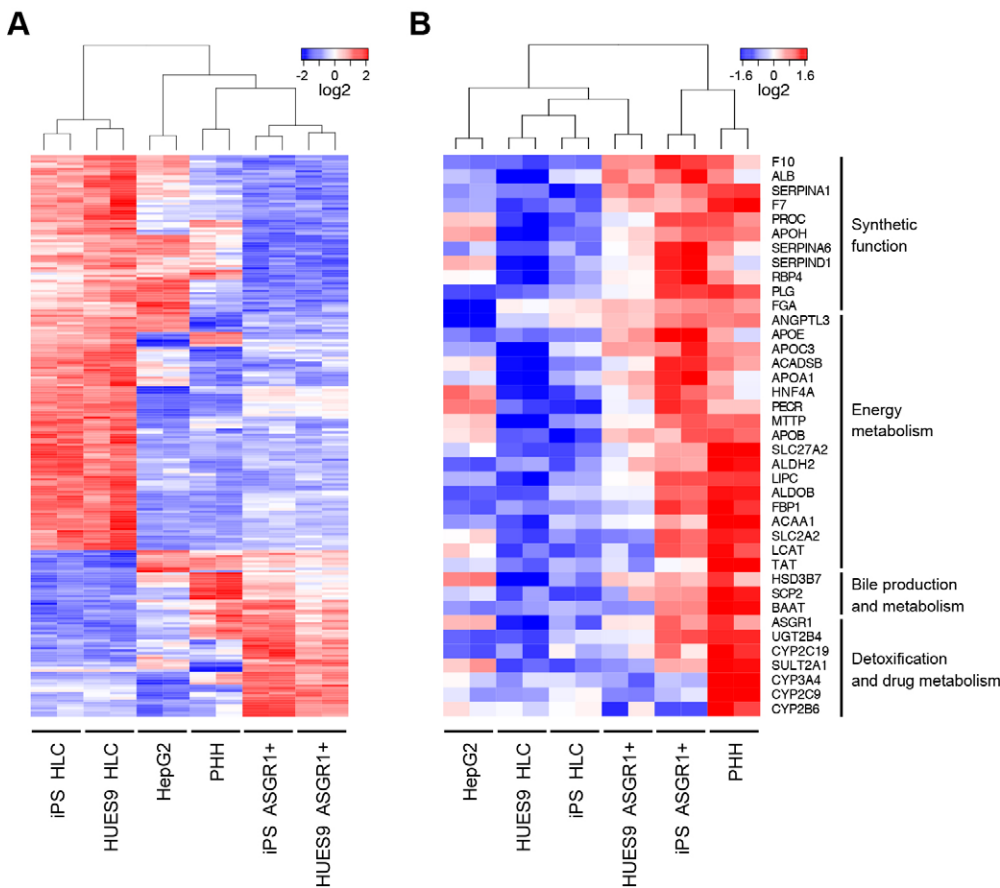
Fig. 3. Global transcriptional analysis shows that ASGR1-positive cells share a distinct transcriptional profile and are more similar than unsorted HLCs to adult hepatocytes. (A) ASGR1-positive cells and HLCs differentiated from two different hPSC lines were compared with HepG2 hepatoma cells and adult primary human hepatocytes (PHHs) using microarrays. Shown is a heatmap of hierarchical clustering performed on genes differentially expressed more than 2-fold between ASGR1-positive cells and HLCs at a 5% FDR. 226 probe sets were differentially expressed greater than 2-fold between ASGR1-positive and unsorted HLCs at 5% FDR; 67 upregulated and 159 downregulated in ASGR1-positive versus unsorted HLCs. (B) Heatmap and hierarchical clustering of a panel of genes related to characteristic hepatic functions across the same samples as in A. Blue, below-average expression, red, above-average expression.

metabolism (including lipid and carbohydrate metabolism and lipoprotein processing), bile production and metabolism, and detoxification and drug metabolism (including metabolism of xenobiotics). The majority of these genes were expressed more highly in ASGR1-positive cells than in unsorted HLCs (Fig. 3B). Hierarchical clustering based on the expression of these hepatic functional genes suggested that ASGR1-positive cells are more similar than HLCs to PHHs (Fig. 3B). It should be noted that this trend is particularly pronounced for genes related to energy metabolism and systemic function in comparison with genes related to detoxification. Finally, we further verified that ASGR1-positive cells are more similar than unsorted HLCs to hepatocytes using gene set enrichment analysis (GSEA) (Subramanian et al., 2005). We found that 346 of 437 liver-enriched genes (79.2%) were more highly expressed in ASGR1-positive cells (Fig. S3E). We have detailed the subsets of liver-enriched genes that are both upregulated and downregulated in ASGR1-positive sorted HLCs versus unsorted HLCs in Table S1.

Replating ASGR1-enriched HLCs
To facilitate functional studies of ASGR1-positive HLCs, we optimized replating HLCs following enrichment of ASGR1-positive cells by magnetic-activated cell sorting (MACS). ASGR1 MACS-enriched HLCs adhered to standard collagen-coated 24-well plates. We examined the expression of lineage and functional hepatocyte markers in replated HLCs differentiated from hESCs and hiPSCs and found that replated cells were positive for these markers as determined by immunofluorescence (Fig. 4A) and qPCR (Fig. S4A). This result was replicated with several hPSC lines. Finally, we assessed representative hepatocyte cellular functions in

replated HLCs in comparison to unsorted HLCs and PHHs. ALB secretion, urea secretion and CYP3A4 activity (representing secretory and detoxification functions of the liver) were significantly increased in replated HLCs versus standard unsorted HLCs (Fig. 4B). As anticipated based on prior characterization of hPSC-derived HLCs, these activities were substantially higher in PHHs. As with the dedifferentiation of primary hepatocytes in cell culture (Miyazaki et al., 1981; Rowe et al., 2010), replated ASGR1-positive HLCs dedifferentiate after 96 h and at this point no longer express the marker genes *AFP*, *FGA*, *AAT*, *ALB*, *TF* or *APOA1* (Fig. S4A) and secrete diminished quantities of ALB (Fig. S4B).

Prospective isolation of hepatocytes from heterogeneous HLC cultures based on ASGR1 surface expression is a viable solution to the problem of variable and incomplete HLC differentiation. We have shown for the first time that ASGR1, an established liver-specific protein, is expressed by a subset of ALB-positive hepatocytes upon HLC differentiation. ASGR1 FACS can be used to isolate a population of cells that express hepatocyte functional markers (*ALB* and *AAT*) even when the overall differentiation efficiency is low. ASGR1-positive sorting addresses both the impurity of HLC differentiation cultures as well as inter-cell line variability in differentiation efficiency, both of which present limitations to performing *in vitro* genetic studies using HLCs. ASGR1 localization at the plasma membrane allows sorting without fixation, making this protocol ideal for the isolation of nucleic acid and protein from purified cells. MACS and replating of ASGR-positive HLCs eliminates the variability commonly encountered during functional studies of differentiated HLCs. This strategy ensures uniformity of cellular activities in comparison to unpurified
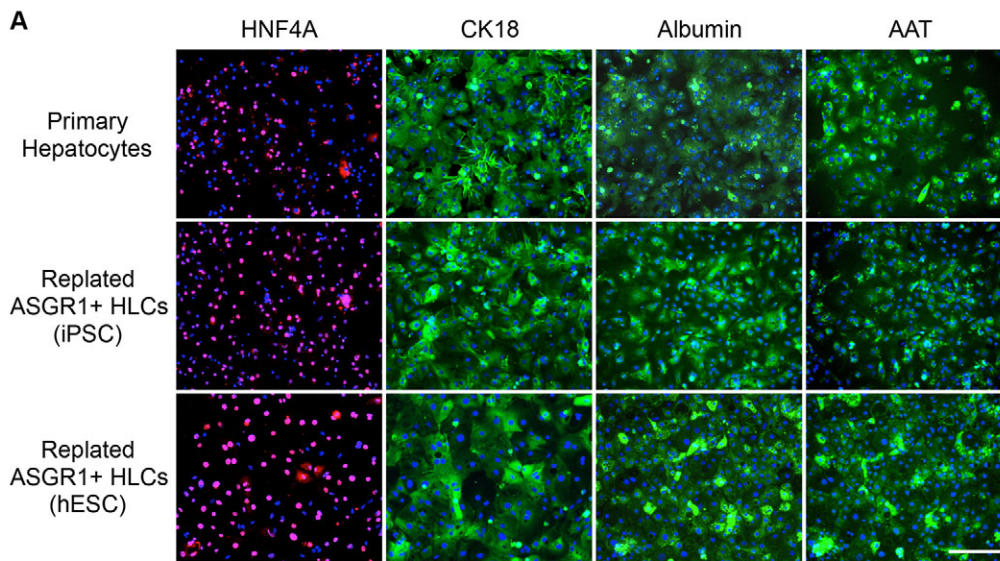
Fig. 4. HLCs can be replated following ASGR1 MACS enrichment and retain hepatocyte characteristics. (A) Immunocytochemical staining for hepatocyte markers in PHHs and replated ASGR1 MACS-enriched HLCs. CK18, cytokeratin 18 (keratin 18, type I). Staining was performed 72 h after replating. Scale bar: 100 µm. (B) Representative assays of hepatocyte cellular functions. Assays were performed at the following time points: unsorted HLCs, day 28 of differentiation; replated HLCs, 72 h after replating on day 25 of differentiation; PHHs, 48 h after plating. $n=4$ per cell line for HLCs and $n=6$ per cell line for replated HLCs. Cryopreserved PHHs were thawed and plated ($n=4$). Error bars represent s.e.m. $**P<0.01$, $***P<0.001$, Student's t-test.
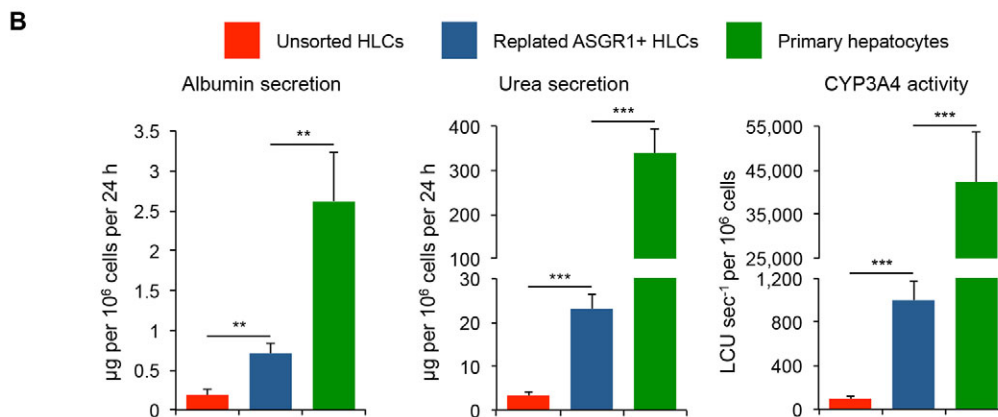
cells. In conclusion, purification of ASGR1-positive cells could be generally applied to isolate HLCs differentiated from hPSCs.

MATERIALS AND METHODS
Cell culture
Two hESC lines (HUES1 and HUES9; Cowan et al., 2004) and two hiPSC lines (1016 and FHS-1) were used. HUES1 and HUES9 cells are part of the NIH hESC registry; 1016 and FHS-1 were derived by the Harvard University Induced Pluripotent Stem Cell Core Facility using retroviral and Sendai viral reprogramming, respectively. Cryopreserved PHHs (HMCPMS lot no. Hu8138) were cultured according to the manufacturer's instructions (Life Technologies). All cell lines were routinely tested for mycoplasma contamination. All ESC lines were maintained in accordance with ESCRO guidelines and iPSC lines were reprogrammed with full consent of donors.

Differentiation of hESCs and iPSCs into HLCs
Media
Basal differentiation medium (BDM): RPMI-1640 (Corning) plus B27 supplement plus penicillin/streptomycin (100 U/ml penicillin, 100 µg/ml streptomycin, final concentration) (Thermo Scientific). Definitive endoderm (DE) medium: BDM with 100 ng/ml activin A and 3 µM CHIR99021. Hepatic endoderm (HE) medium: BDM with 5 ng/ml basic fibroblast growth factor (bFGF, also known as FGF2), 20 ng/ml bone morphogenetic protein 4 (BMP4) and 0.5% DMSO. IMH medium: BDM with 20 ng/ml hepatocyte growth factor (HGF) and 0.5% DMSO. Mature hepatocyte (MH) medium: hepatocyte basal medium (HBM) (Lonza) with SingleQuots added (Lonza), as well as 20 ng/ml HGF, 20 ng/ml oncostatin M, 100 nM dexamethasone and 0.5% DMSO.

Plating and differentiation
Day 1: cultures of ESCs/iPSCs were split and plated at a density of 3×10^4 cells/cm^2 in mTESR (Stem Cell Technologies) with 4 µM ROCK inhibitor Y27632. Plating density may have to be optimized for each cell line. Days 2-4: cells were treated with DE medium. Days 5-9: cells were treated with HE medium for 5 days. Days 10-14: cells were treated with IMH for 5 days. Days 15-27: cells were treated with MH medium for 10-12 days. The medium was changed daily throughout differentiation. All cell sorting and staining experiments for the HLC stage were performed at day 25 of differentiation, whereas experiments studying the IMH stage were performed at day 14 of differentiation.

Immunocytochemistry
The following primary and secondary antibodies were used for immunocytochemical staining: AAT (MA1-90438, Thermo Scientific), ALB (A80-129A, Bethyl), ASGR1 (clone 8D7, BD Biosciences), CK18 (ab82254, Abcam) and HNF4α (ab92378, Abcam) primary antibodies at 1:250, and donkey anti-goat IgG Alexa Fluor 555 (A-21432, Thermo Scientific), donkey anti-mouse IgG Alexa Fluor 488 (A-21202, Thermo Scientific) and donkey anti-rabbit IgG Alexa Fluor 488 (A-21206, Thermo Scientific) secondary antibodies (all Life Technologies) at 1:1000. Hoechst (1:5000; Life Technologies) was used for nuclear staining. Staining in unsorted HLCs was visualized using an LSM 700 confocal microscope (Carl Zeiss) and an inverted Eclipse Ti microscope (Nikon).

Intracellular flow cytometry
For flow cytometry analysis, differentiated cells were fixed and stained using the Cytofix/Cytoperm Kit (BD) following the manufacturer's instructions.

The primary and secondary antibodies described above were used at experimentally optimized dilutions. Additional antibodies used in flow cytometry experiments were mouse IgG1 isotype control (554121, BD; 1:20), donkey anti-mouse IgG Alexa Fluor 594 (A-21203, Thermo Scientific; 1:500), donkey anti-goat IgG Alexa Fluor 488 (ab150129, Abcam; 1:500) and donkey anti-goat IgG Alexa Fluor 647 (A-21447, Thermo Scientific; 1:500). Cells were analyzed using an LSR II cytometer (BD) and FlowJo software.

FACS of HLCs
After day 12 of feeding with MH medium, HLCs were washed with Dulbecco's phosphate-buffered saline (DPBS) and treated with 0.25% trypsin-EDTA. Cells were treated with a Stempro EZ Passage passaging tool (Life Technologies) and incubated at 37°C for 15 min. After dissociation, remaining cells were gently scraped from the dish and filtered through a 100 μm mesh. Cells were stained with a PE-conjugated ASGR1 antibody (8D7, BD, 563655) or a PE-conjugated mouse IgG1κ isotype control antibody (BD, 551436) according to manufacturer's dilution instructions. After incubation, cells were washed twice with PBS. Alternatively, in some experiments cells were stained with unconjugated ASGR1 primary antibody or mouse IgG1 isotype control, washed, and stained with donkey anti-mouse IgG Alexa Fluor 488 secondary antibody (as above). ASGR1-positive cells were purified by FACS using a FACSAria II (BD).

RNA isolation and qRT-PCR
RNA was isolated using Trizol (Life Technologies). qPCR was performed using TaqMan Gene Expression Master Mix and TaqMan gene expression assays (Life Technologies) for the following: *RPLP0* (reference control gene), *AFP*, *CYP3A7*, *FGA*, *ALB*, *AAT*, *TF* and *APOA1*.

Microarray gene expression profiling
U219 gene expression arrays (Affymetrix) were used according to the manufacturer's instructions. These data have been uploaded to Gene Expression Omnibus (GEO) under accession number GSE77086.

Preprocessing and hierarchical clustering
Microarrays were normalized and background corrected using the robust multi-array (RMA) method in the Bioconductor affy package in R v3.1.2 (Gautier et al., 2004). Normalized array values were reported on a $\log_2$ scale and probe sets with low expression values across all samples ($\log_2$ intensity <2.5) were filtered out. Unsupervised hierarchical clustering was performed using the hclust function in R. The statistical significance of clustering results was estimated by multiscale bootstrap resampling using the pvclust function with 10,000 iterations.

Standard differential expression analysis and heatmap generation
Analysis was performed using Transcriptome Analysis Console software (Affymetrix). FDR-adjusted *P*-values were calculated based on the Benjamini-Hochberg method and 5% FDR cutoff was used. Heatmaps were created using the heatmap.2 function in R, with accompanying dendrograms drawn based on Euclidean distance.

Paired-sample differential expression analysis, functional enrichment testing of differentially expressed genes and GSEA
The R/Bioconductor limma package was used to fit linear models for each gene, utilizing a paired-sample design. Moderated *t*-statistics, log fold change and *P*-values were calculated. To correct for multiple hypothesis testing, FDR-adjusted *P*-values were calculated by the Benjamini-Hochberg method. Probe sets were filtered by FDR<5% and fold change >2 (1079 probe sets). Functional enrichment analysis was performed using the PANTHER resource. GSEA (Subramanian et al., 2005) was performed using GSEA software (Broad Institute, Cambridge, MA, USA) and a list of liver-enriched genes (Yang et al., 2011).

Analysis of published gene expression data
Published microarray gene expression data were obtained from BioGPS.org and the GEO database: accession numbers GSE25417 (DeLaForest et al., 2011) and GSE1133 (Su et al., 2004). Analysis and heatmap generation were conducted using GENE-E software (Broad Institute).

ASGR1 MACS and replating of HLCs
Cells were released as described for flow cytometry analysis. After blocking, anti-ASGR1 antibody (8D7, BD; 1:150) was added. After incubation on ice for 30 min, cells were pelleted (5 min, 233 g) and resuspended in cold MACS buffer with anti-mouse IgG microbeads (1:20; Miltenyi Biotec). After incubation on ice for 30 min, cells were washed and then passed through a 100 μM filter. Cells were then sorted using an autoMACS Pro separator (Miltenyi Biotec). After sorting, cells were pelleted and resuspended in HLC replating medium: hepatocyte basal medium with SingleQuots supplements, HGF (20 ng/ml), dexamethasone (100 nM), ROCK inhibitor (4 μM), penicillin/streptomycin and gentamicin (50 μg/ml). Cells were plated on collagen-coated 24-well culture dishes (A1142802, Thermo Scientific) by centrifugation of the plate at 100 RCF for 15 min at 37°C. Cells were replated at 15,000 cells per cm^2 and thereafter maintained in HLC replating medium without ROCK inhibitor. Cells were used in functional assays no later than 72 h after replating, owing to cell dedifferentiation during prolonged culture.

Cellular assays of hepatocyte functions
Cellular assay results were normalized to the number of live cells as determined by hemocytometer cell counting with Trypan Blue staining. ALB secretion was quantified using an enzyme-linked immunosorbent assay (Bethyl Laboratories, E80-129) according to the manufacturer's instructions. Urea production was quantified using the QuantiChrom Urea Assay Kit (BioAssay Systems) following the manufacturer's instructions. Cytochrome activity was quantified using the P450-Glo CYP3A4 assay (Luc-PFBE) (Promega) following the manufacturer's instructions.

Statistical analysis
Statistical significance was assessed using standard Student's *t*-test (two-tail); $P<0.05$ was considered statistically significant. Experiments were performed in triplicate unless otherwise noted.

Competing interests
The authors declare no competing or financial interests.

Author contributions
D.T.P. and C.R.W. designed and performed experiments and wrote the manuscript. C.A.H. and M.F. designed and performed experiments. F.X. performed experiments. C.E.B. reprogrammed iPSC lines. K.M. supported D.T.P. C.A.C. designed experiments and guided the study.

Data availability
Microarray data are available at Gene Expression Omnibus under accession number GSE77086.

Supplementary information
Supplementary information available online at
http://dev.biologists.org/lookup/suppl/doi:10.1242/dev.132209/-/DC1

References
Ashwell, G. and Morell, A. G. (1974). The role of surface carbohydrates in the hepatic recognition and transport of circulating glycoproteins. *Adv. Enzymol. Relat. Areas Mol. Biol.* **41**, 99-128.
Basma, H., Soto-Gutiérrez, A., Yannam, G. R., Liu, L., Ito, R., Yamamoto, T., Ellis, E., Carson, S. D., Sato, S., Chen, Y. et al. (2009). Differentiation and transplantation of human embryonic stem cell–derived hepatocytes. *Gastroenterology* **136**, 990-999.e4.
Bock, C., Kiskinis, E., Verstappen, G., Gu, H., Boulting, G., Smith, Z. D., Ziller, M., Croft, G. F., Amoroso, M. W., Oakley, D. H. et al. (2011). Reference Maps of

human ES and iPS cell variation enable high-throughput characterization of pluripotent cell lines. *Cell* **144**, 439-452.

Cowan, C. A., Klimanskaya, I., McMahon, J., Atienza, J., Witmyer, J., Zucker, J. P., Wang, S., Morton, C. C., McMahon, A. P., Powers, D. et al. (2004). Derivation of embryonic stem-cell lines from human blastocysts. *N. Engl. J. Med.* **350**, 1353-1356.

DeLaForest, A., Nagaoka, M., Si-Tayeb, K., Noto, F. K., Konopka, G., Battle, M. A. and Duncan, S. A. (2011). HNF4A is essential for specification of hepatic progenitors from human pluripotent stem cells. *Development* **138**, 4143-4153.

Gautier, L., Cope, L., Bolstad, B. M. and Irizarry, R. A. (2004). affy–analysis of Affymetrix GeneChip data at the probe level. *Bioinformatics* **20**, 307-315.

Kajiwara, M., Aoi, T., Okita, K., Takahashi, R., Inoue, H., Takayama, N., Endo, H., Eto, K., Toguchida, J., Uemoto, S. et al. (2012). Donor-dependent variations in hepatic differentiation from human-induced pluripotent stem cells. *Proc. Natl. Acad. Sci. USA* **109**, 12538-12543.

Khetani, S. R. and Bhatia, S. N. (2008). Microscale culture of human liver cells for drug development. *Nat. Biotechnol.* **26**, 120-126.

Knowles, B. B., Howe, C. C. and Aden, D. P. (1980). Human hepatocellular carcinoma cell lines secrete the major plasma proteins and hepatitis B surface antigen. *Science* **209**, 497-499.

Li, J., Chen, L., Zhang, X., Zhang, Y., Liu, H., Sun, B., Zhao, L., Ge, N., Qian, H., Yang, Y. et al. (2014). Detection of circulating tumor cells in hepatocellular carcinoma using antibodies against asialoglycoprotein receptor, carbamoyl phosphate synthetase 1 and pan-cytokeratin. *PLoS ONE* **9**, e96185.

Mallanna, S. K. and Duncan, S. A. (2013). Differentiation of hepatocytes from pluripotent stem cells. *Curr. Protoc. Stem Cell Biol.* **26**, 1G.4.1-1G.4.13.

Mi, H., Muruganujan, A. and Thomas, P. D. (2013). PANTHER in 2013: modeling the evolution of gene function, and other gene attributes, in the context of phylogenetic trees. *Nucleic Acids Res.* **41**, D377-D386.

Miyazaki, K., Takaki, R., Nakayama, F., Yamauchi, S., Koga, A. and Todo, S. (1981). Isolation and primary culture of adult human hepatocytes: ultrastructural and functional studies. *Cell Tissue Res.* **218**, 13-21.

Osafune, K., Caron, L., Borowiak, M., Martinez, R. J., Fitz-Gerald, C. S., Sato, Y., Cowan, C. A., Chien, K. R. and Melton, D. A. (2008). Marked differences in differentiation propensity among human embryonic stem cell lines. *Nat. Biotechnol.* **26**, 313-315.

Pagliuca, F. W., Millman, J. R., Gürtler, M., Segel, M., Van Dervort, A., Ryu, J. H., Peterson, Q. P., Greiner, D. and Melton, D. A. (2014). Generation of functional human pancreatic beta cells in vitro. *Cell* **159**, 428-439.

Rowe, C., Goldring, C. E. P., Kitteringham, N. R., Jenkins, R. E., Lane, B. S., Sanderson, C., Elliott, V., Platt, V., Metcalfe, P. and Park, B. K. (2010). Network analysis of primary hepatocyte dedifferentiation using a shotgun proteomics approach. *J. Proteome Res.* **9**, 2658-2668.

Schwartz, A. L., Marshak-Rothstein, A., Rup, D. and Lodish, H. F. (1981). Identification and quantification of the rat hepatocyte asialoglycoprotein receptor. *Proc. Natl. Acad. Sci. USA* **78**, 3348-3352.

Schwartz, R. E., Fleming, H. E., Khetani, S. R. and Bhatia, S. N. (2014). Pluripotent stem cell-derived hepatocyte-like cells. *Biotechnol. Adv.* **32**, 504-513.

Si-Tayeb, K., Noto, F. K., Nagaoka, M., Li, J., Battle, M. A., Duris, C., North, P. E., Dalton, S. and Duncan, S. A. (2010). Highly efficient generation of human hepatocyte-like cells from induced pluripotent stem cells. *Hepatology* **51**, 297-305.

Su, A. I., Wiltshire, T., Batalov, S., Lapp, H., Ching, K. A., Block, D., Zhang, J., Soden, R., Hayakawa, M., Kreiman, G. et al. (2004). A gene atlas of the mouse and human protein-encoding transcriptomes. *Proc. Natl. Acad. Sci. USA* **101**, 6062-6067.

Subramanian, A., Tamayo, P., Mootha, V. K., Mukherjee, S., Ebert, B. L., Gillette, M. A., Paulovich, A., Pomeroy, S. L., Golub, T. R., Lander, E. S. et al. (2005). Gene set enrichment analysis: a knowledge-based approach for interpreting genome-wide expression profiles. *Proc. Natl. Acad. Sci. USA* **102**, 15545-15550.

Takayama, K., Morisaki, Y., Kuno, S., Nagamoto, Y., Harada, K., Furukawa, N., Ohtaka, M., Nishimura, K., Imagawa, K., Sakurai, F. et al. (2014). Prediction of interindividual differences in hepatic functions and drug sensitivity by using human iPS-derived hepatocytes. *Proc. Natl. Acad. Sci. USA* **111**, 16772-16777.

Yang, X., Ye, Y., Wang, G., Huang, H., Yu, D. and Liang, S. (2011). VeryGene: linking tissue-specific genes to diseases, drugs, and beyond for knowledge discovery. *Physiol. Genomics* **43**, 457-460.
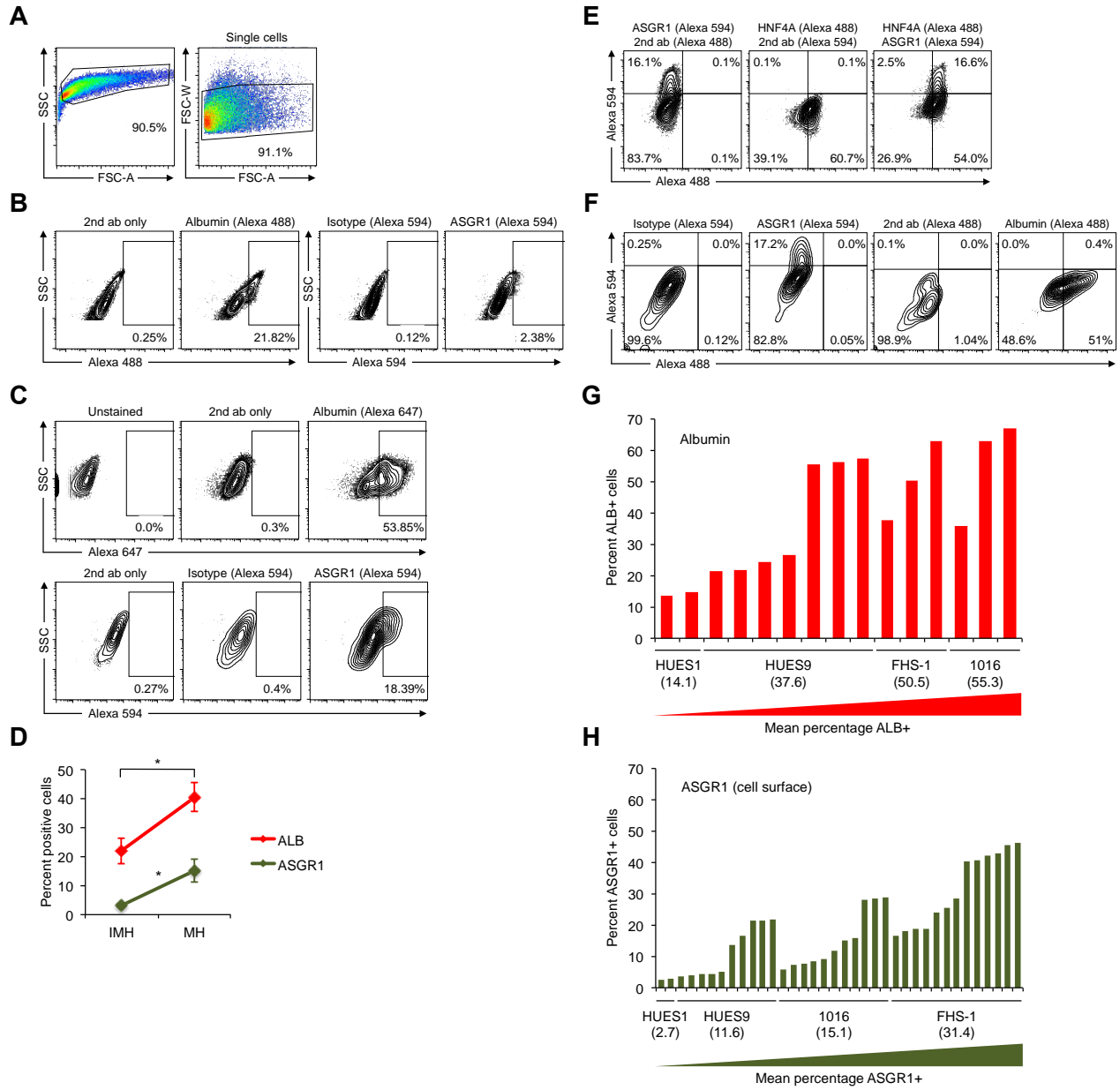
Figure S1. Flow cytometry analysis of HLC differentiation, related to Figure 1. (A) Gating used for flow cytometry analyses; single cells were defined by FSC-A/SSC (cell size and granularity) and FSC-W (cell width) to exclude debris, cell clumps, and doublets. (B) Albumin and ASGR1 expression after the IMH differentiation stage with corresponding staining controls. Alexa 488 and Alexa 594 conjugated secondary antibodies were used with albumin and ASGR1 primary antibodies respectively; gating for albumin and ASGR1 positive cells was performed using secondary-only and isotype-control staining conditions

respectively. (C) Albumin and ASGR1 expression after the MH differentiation stage with corresponding staining controls. Alexa 647 and Alexa 594 conjugated secondary antibodies were used with albumin and ASGR1 primary antibodies respectively; gating for albumin and ASGR1 positive cells was performed using secondary-only and isotype-control staining conditions respectively. A secondary-only staining control is also shown for ASGR1. (D) Kinetics of albumin and ASGR1 expression during the final stages of HLC differentiation as determined by intracellular flow cytometry. Shown are mean percent positive cells at the IMH and MH stages based on multiple independent differentiations (n = 5 - 15 replicates per marker, per stage). Error bars represent s.e.m. Asterisks indicate statistically significant differences in mean percentage of positive cells at the IMH and MH stages for each marker by Student's *t*-test. *, $P < 0.05$. (E) Flow cytometry analysis of ASGR1 and HNF4A co-expression with staining controls. Alexa 594 and Alexa 488 conjugated secondary antibodies were used for ASGR1 and HNF4A staining respectively. Gating was performed based on secondary-only (fluorescence minus one) staining conditions. (F) Flow cytometry analysis of ASGR1 and albumin co-expression with staining controls. Alexa 594 and Alexa 488 conjugated secondary antibodies were used for ASGR1 and albumin staining respectively. Gating for ASGR1 and albumin positive cells was performed based on isotype-control and secondary-only staining conditions respectively. (G-H) Efficiency of HLC differentiation with four different hPSC lines over multiple independent experiments. Shown are percent albumin-positive (G) and surface ASGR1-positive (H) cells determined by flow cytometry analysis after the MH differentiation stage, illustrating a range of differentiation efficiencies.
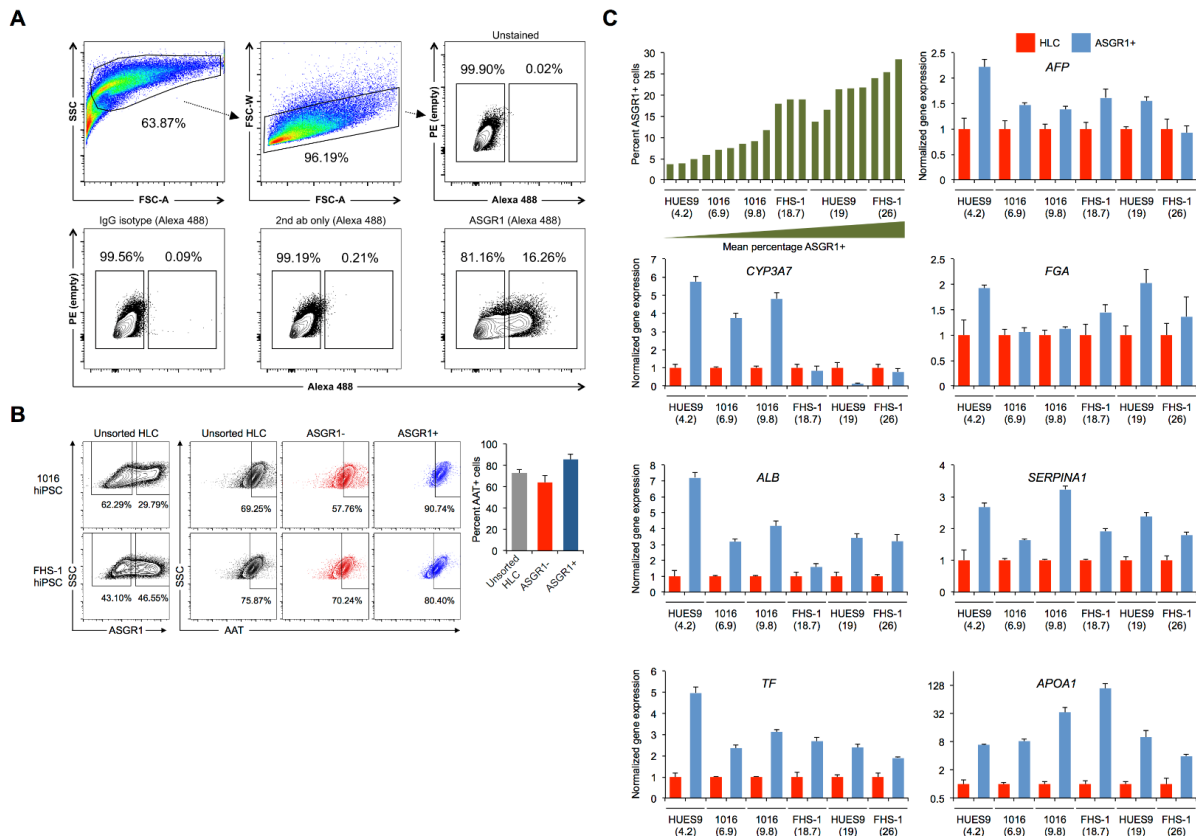
Figure S2. Detailed results of ASGR1 FACS and hepatocyte marker gene expression analysis, related to Figure 2. (A) Strategy and staining controls for FACS isolation of ASGR1+ HLCs. Shown are results of a representative differentiation and FACS experiment. (B) Left: two different hPSC lines were differentiated to HLCs. The percentage of cells expressing the hepatocyte marker alpha-1 antitrypsin (AAT) among unsorted HLCs, surface ASGR1-negative cells, and surface ASGR1-positive cells was quantified by intracellular flow cytometry. Right: mean percent AAT-positive cells by flow cytometry, among unsorted HLCs, surface ASGR1-negative cells, and surface ASGR1-positive cells (n = 2 differentiations). Error bars represent s.e.m. (C) ASGR1 FACS and hepatocyte marker gene expression analysis by qRT-PCR. Gene expression data is displayed as a heatmap in Figure 2C. Three different hPSC lines were differentiated to HLCs, with two independent differentiations performed per cell line (differentiations performed in triplicate or greater, $n = 6 – 8$ biological replicates per cell line). Data are arranged according to mean percent ASGR1+ cells obtained in each differentiation. Green bars: percentage surface ASGR1+ cells after the MH

differentiation stage. All other graphs show qRT-PCR gene expression analysis in unsorted HLCs ("HLC," red bars) and ASGR1+ cells ("ASGR1+," blue bars) isolated by FACS. Expression levels are relative to *RPLP0* expression; gene expression levels in ASGR1+ cells were normalized to level in unsorted HLCs. Shown are normalized mean expression levels for each differentiation ($n = 3 - 5$ paired biological replicates per differentiation). Error bars represent s.e.m.

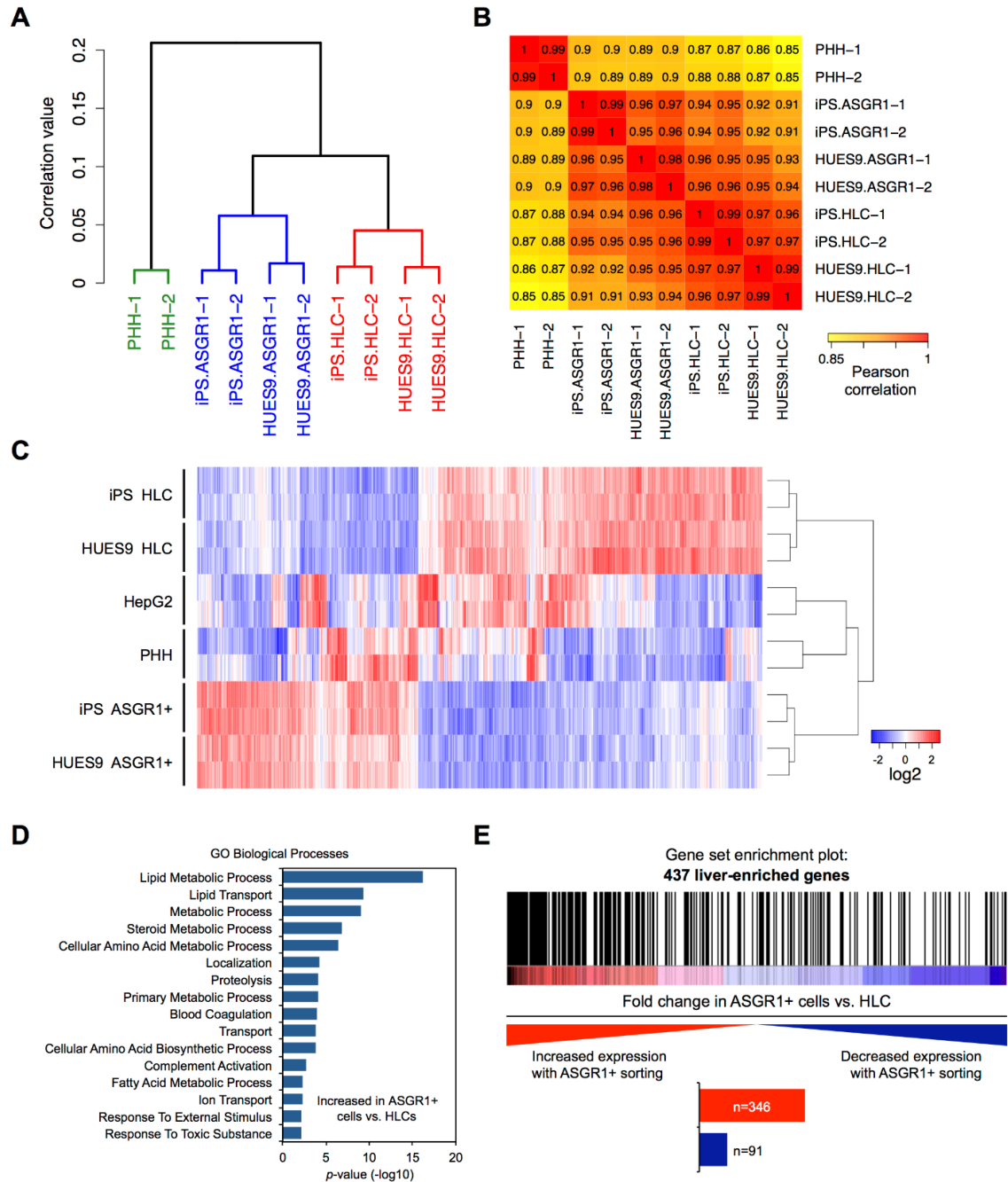**Figure S3. Additional analyses of microarray gene expression profiling data from ASGR1-positive cells, unsorted HLCs, primary human hepatocytes, and HepG2 hepatoma cells, related to figure 3.** (A) Hierarchical clustering of ASGR1-positive, HLC, and PHH samples based on all genes measured by transcriptional microarray and expressed above background. (B) Heatmap showing pairwise Pearson correlation values for ASGR1-

positive, HLC, and PHH samples based on the same expression data used in part A. Yellow, orange, and red color denotes lower, intermediate, and higher correlation respectively. (C) Heatmap of hierarchical clustering performed on all genes differentially expressed between ASGR1-positive cells and HLCs at a 5% FDR. Blue, below average expression, red, above average expression. 813 probesets differentially expressed between ASGR1+ and unsorted HLC at 5% FDR; 318 upregulated and 495 downregulated in ASGR1+ vs. unsorted HLCs respectively. (D) Functional enrichment analysis of genes differentially expressed in ASGR1-positive cells relative to HLCs. (E) Gene set enrichment analysis (GSEA). Microarray gene expression data was arranged based on greater average expression in ASGR1-positive cells (red color) or unsorted HLCs (blue color). Vertical black bars represent genes within the liver-enriched gene set.
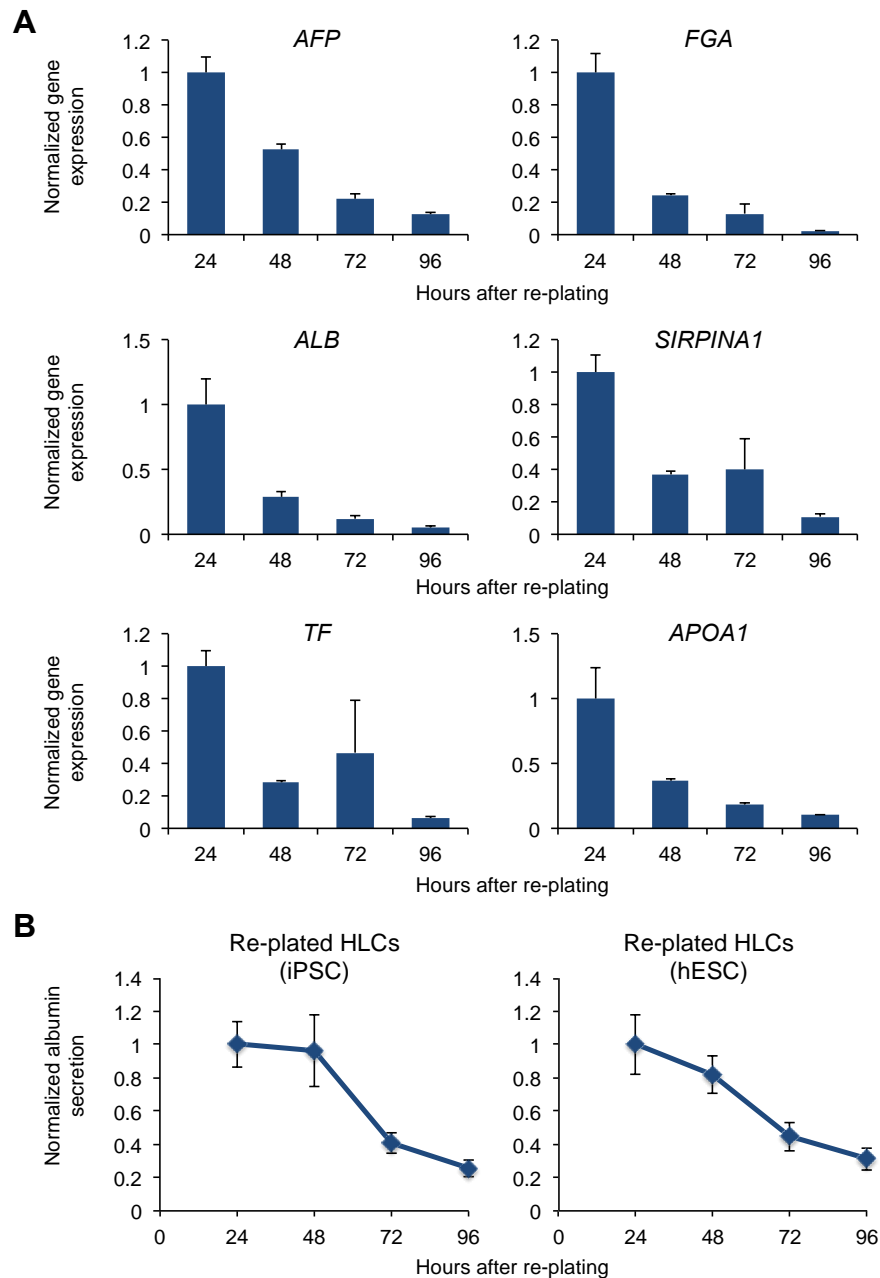
Figure S4. Hepatocyte marker gene expression and albumin secretion declines as anticipated following re-plating of ASGR1 MACS-enriched HLCs. (A) Changes in hepatocyte marker gene expression over time were determined by qRT-PCR after re-plating HLCs differentiated from a representative hESC line. Gene expression levels were calculated relative to *RPLP0* expression and normalized to gene expression level at 24 hours post re-plating for each gene (*n* = 3 differentiation wells per time point). Error bars represent s.e.m. (B)

Quantification of albumin secretion by ELISA following re-plating of HLCs differentiated from two hPSC lines. Albumin concentration at the indicated time points were calculated using a standard curve and normalized to the level at 24 hours post re-plating for each cell line (n = 3 differentiation wells per cell line, per time point). Medium was collected after 24 hours in culture for each time point. Error bars represent s.e.m.

Table S1. Distribution of liver-enriched genes in gene set enrichment analysis (GSEA) comparing ASGR1+ cells and unsorted HLCs, related to Figure S3E.

Subset of liver-enriched genes with greater expression in ASGR1+ cells. 205 genes contributed most strongly to the enrichment result (core enrichment). 346 of 437 genes had greater expression in ASGR1+ cells vs. unsorted HLCs.						Liver-enriched genes with lower expression in ASGR1+ cells. 91 of 437 genes had lower expression in ASGR1+ cells vs. unsorted HLCs		
AADAC	ASGR1	FBP1	LEPR	SEPHS2	TTR	ABCB4	FMO4	SEC14L2
ABCG8	ASGR2	FETUB	LIPC	SERPINA10	UGT2B4	ABCG5	GCGR	SEC14L4
ACAA1	ASS1	FGA	MAT1A	SERPINA4	UGT3A1	ACAT2	GHR	SLCO1B1
ACAA2	ATF5	FGB	METTL7B	SERPINA6	VTN	ACOT12	GLS2	SOD1
ACADSB	AZGP1	FGFR4	MTHFS	SERPINA7	ZNHIT1	ANXA10	GLT1D1	SPP2
ACAT1	BAAT	FGG	MTTP	SERPINC1		APOC4	GNE	STEAP3
ACMSD	BPHL	FGL1	MUT	SERPIND1		AQP9	GNPNAT1	THPO
ACOX1	BRP44	FMO5	NAT8	SERPINF2		AS3MT	GPR126	TNFSF14
ACOX2	C1S	G6PC	NEK6	SERPING1		ATF7IP2	GRHPR	TUBB1
ACSL1	C5	GATM	NIPSNAP1	SHMT1		BCO2	GSTZ1	UROC1
ACY1	C6	GC	NIT2	SHMT2		C4BPA	GYS2	ZNF281
ADH1A	CD302	GCHFR	OIT3	SLC10A1		C4BPB	HAGH	
ADH6	CDO1	GGH	ORM1	SLC13A5		CCL16	HAMP	
ADK	CFH	GSTO1	OTC	SLC22A7		CD5L	HLF	
AFF4	CFI	HABP2	PAH	SLC22A9		CDC37L1	HPS3	
AFM	CIDEB	HMGCL	PCBD1	SLC25A13		CES1	HSD11B1	
AGTR1	CLDN1	HMGCS2	PCCB	SLC27A2		CES2	IBTK	
AGXT	CPB2	HNF4A	PCK2	SLC2A2		CFP	IGFALS	
AGXT2	CPN1	HP	PEBP1	SLC30A1		CLEC4M	ITIH4	
AHSG	CPN2	HPD	PECR	SLC35D1		COLEC11	KMO	
AIG1	CPS1	HPN	PEMT	SLC38A3		CP	LARP4	
AKR1A1	CREB3L3	HPX	PGRMC1	SLC38A4		CRP	LECT2	
AKR1D1	CRYL1	HRSP12	PHYH	SLC39A14		CTH	LPIN2	
ALAS1	CYB5A	HSD17B4	PIPOX	SLC41A2		CYP1A2	MAMDC4	
ALB	CYP3A7	HSD3B7	PKLR	SLC43A1		CYP26A1	MASP1	
ALDH6A1	CYP4A11	HSPE1	PLA2G12B	SLCO2B1		CYP2A6	MASP2	
ALDH8A1	CYP4V2	ID2	PLG	SORD		CYP2B7P1	MBL2	
ALDOB	CYP8B1	IGFBP1	PNPLA3	SPRYD4		CYP2C8	MCL1	
AMBP	DCXR	IL1RAP	PRAP1	ST6GAL1		CYP2D6	MTHFD1	
ANG	DDT	INHBE	PRDX4	SULT2A1		CYP2E1	MYO1B	
ANGPTL3	DECR1	INSIG1	PROC	TAT		CYP39A1	N4BP2L1	
APOA1	EPHX1	ITIH1	PROS1	TDO2		CYP4A22	PHLDA1	
APOA2	ETFB	ITIH2	PROX1	TFR2		DEFB123	PLGLB2	
APOB	F10	KHK	PROZ	TM4SF4		DEPDC7	PON1	
APOC2	F13B	KLB	PXMP2	TM4SF5		DHRS1	PON3	
APOC3	F2	KLKB1	RBP4	TMEM176A		DMGDH	PPAPDC2	
APOE	F5	KNG1	RCL1	TMEM176B		ERRFI1	PZP	
APOH	F7	LASS2	SAA4	TMEM56		ETFDH	RTP3	
APOM	F9	LBP	SC5DL	TMPRSS6		FAM167B	SCUBE3	
ARG1	FAM96A	LCAT	SCP2	TP53INP1		FMO3	SDS	